

Uncertainty effects on lifetime structural performance of cable-stayed bridges

Fabio Biondini^{a,*}, Dan M. Frangopol^b, Pier Giorgio Malerba^a

^a *Department of Structural Engineering, Politecnico di Milano P.za L. da Vinci, 32–20133 Milan, Italy*

^b *Department of Civil and Environmental Engineering, Center for Advanced Technology for Large Structural Systems, Imbt Labs, Lehigh University, Bethlehem, PA, USA*

Received 11 May 2007; accepted 10 January 2008

Available online 29 February 2008

Abstract

This paper investigates the time evolution of the uncertainty effects associated with the different parameters defining the probabilistic structural performance of two existing cable-stayed bridges in Italy. The study is developed by using a general methodology for time-variant reliability analysis of concrete structures subjected to diffusive attacks from external aggressive agents. The time evolution of the probabilistic structural performance is analyzed with reference to proper indicators of the nonlinear behavior. The beneficial effects of prescribed rehabilitation interventions are also taken into account. The effects of each random variable on such indicators for both damaged and rehabilitated structures are quantified and compared by means of suitable time-dependent sensitivity factors. The obtained results show that the relative importance of the uncertainty effects associated with each random variable may vary significantly over time, and that this variation is considerably reduced by the adopted rehabilitation interventions.

© 2008 Elsevier Ltd. All rights reserved.

1. Introduction

Inspection and monitoring of existing concrete cable-stayed bridges highlight the noteworthy sensitivity of this kind of structures to the damaging effects associated with diffusive attacks from environmental aggressive agents. These effects usually involve a progressive deterioration of concrete and corrosion of reinforcement, and may lead to a significant variation of structural performance over time. As a consequence, maintenance and rehabilitation interventions are often required to restore, partially or totally, the original performance of the undamaged structure [5].

The decision making process aimed to plan a maintenance activity and properly design eventual rehabilitation interventions must be supported by a robust lifetime reliability analysis, able to account for the uncertainties affecting the structural performance [11,1,10,7,9,12]. However, for concrete structures the number of involved uncertain parameters is usually large, and

probabilistic evaluations may become very complex. This aspect is particularly emphasized when full nonlinear analyses are required to investigate the time-variant structural performance. A possible way to reduce the complexity of the reliability problem is to consider only a few uncertain parameters as random variables, typically only those which mainly affect the structural response.

In concrete design, the parameters assumed as random variables are generally associated with the material properties, i.e. concrete and steel strengths, while for the other mechanical and geometrical parameters the deterministic nominal values are assumed. For undamaged structures this approach is calibrated by the codes to be on the safe side and is proven to be effective for practical purposes. However, despite the unavoidable sources of structural damage, a design procedure aimed at achieving the required level of structural reliability not only at the initial time, but over the whole expected lifetime of the structure, must consider that the relative importance of the uncertainty effects associated with each design parameter may vary significantly during time.

The results of a preliminary investigation to highlight the time evolution of the uncertainty effects associated with the

* Corresponding author. Tel.: +39 02 2399 4394; fax: +39 02 2399 4220.

E-mail addresses: biondini@stru.polimi.it (F. Biondini), dan.frangopol@lehigh.edu (D.M. Frangopol), malerba@stru.polimi.it (P.G. Malerba).

different parameters which define the structural performance has been presented in [4]. The results of this comparison indicates that the classical view in which the main role in concrete design is played by the uncertainty associated with the material strengths needs to be revisited to account for the effects of the unavoidable sources of structural damage which during time may strongly modify the structural performance.

These aspects are further investigated in the present paper by focusing the attention on the specific case of two existing cable-stayed bridges in Italy [15]. The lifetime structural performance of these bridges is investigated at a cross-sectional level by using a general method for time-variant probabilistic analysis of concrete structures in aggressive environments [2, 3,6]. In this approach the diffusion process is modeled by using a special class of evolutionary algorithms, called cellular automata, and the mechanical damage coupled to diffusion is evaluated by introducing proper material degradation laws. The probabilistic analysis is carried out by Monte Carlo simulation and the corresponding time evolution of the structural performance is investigated with reference to suitable indicators of the nonlinear behavior. The beneficial effects of prescribed rehabilitation interventions on these indicators are also taken into account. The effects of the uncertainty associated with each random variable on such indicators, for both damaged and rehabilitated structures, are finally quantified and compared by means of time-dependent sensitivity factors based on a regression of the simulation results. The obtained results show that the relative importance of the uncertainty effects associated with each random variable may significantly vary over time, and that this variation is considerably reduced by the adopted rehabilitation interventions.

2. Probabilistic lifetime performance of concrete structures

2.1. Concrete structures in aggressive environments

For concrete structures, the diffusive attack of environmental aggressive agents, like sulfate and chloride, may cause deterioration of concrete and corrosion of reinforcement [8]. Such processes involve several factors, including temperature and humidity. Their dynamics are governed by the coupled diffusion process of heat, moisture and various chemical substances. In addition, damage induced by mechanical loading interacts with the environmental factors and accelerates the deterioration process [16,18]. Therefore, a durability analysis of concrete structures in aggressive environments should be able to account for both the diffusion process and the corresponding mechanical damage, as well as for the coupling effects between diffusion, damage and structural behavior. However, the available information about environmental factors and material characteristics is often very limited and the unavoidable uncertainties involved in a detailed and complex modeling may lead to erroneous results. For these reasons, the assessment of the structural lifetime can be more reliably carried out by means of macroscopic models which exploit the power and generality of the basic laws of diffusion to predict the quantitative time-variant response of damaged structural

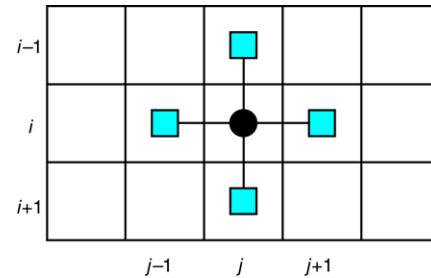


Fig. 1. Neighborhood of a cell (i, j) for a two-dimensional cellular automaton.

systems. Based on these considerations, a general procedure for time-variant probabilistic assessment and lifetime prediction of concrete structures in aggressive environments was proposed [2,3]. In the following the main aspects of the proposed approach applied to reinforced and prestressed concrete cross-sections subjected to the diffusive attacks from environmental aggressive agents are briefly summarized.

2.2. Simulation of the diffusion process

The kinetic process of mass diffusion of chemical components in solids is usually described by using Fick's model [13]:

$$D \nabla^2 C = \frac{\partial C}{\partial t} \quad (1)$$

where $C = C(\mathbf{x}, t)$ is the mass concentration of the aggressive agent at point $\mathbf{x} = (y, z)$ and time t , $D = D(\mathbf{x}, t)$ is the diffusivity coefficient, $\nabla C = \mathbf{grad} C$, and $\nabla^2 = \nabla \cdot \nabla$. To deal with complex geometrical and mechanical boundary conditions, the solution of the previous differential equation requires the use of numerical methods.

In this study, the diffusion equation is effectively solved by using a special class of evolutionary algorithms called cellular automata. In its basic form, a cellular automaton consists of a regular uniform grid of cells with a discrete variable in each cell which can take on a finite number of states [17]. In particular, as demonstrated in the Appendix, Fick's model in two-dimensions can be reproduced by adopting the following evolutionary rule [2]:

$$C_{ij}^{k+1} = \phi_0 C_{ij}^k + \frac{1 - \phi_0}{4} (C_{i,j-1}^k + C_{i,j+1}^k + C_{i-1,j}^k + C_{i+1,j}^k) \quad (2)$$

where the discrete variable $C_{ij}^k = C(\mathbf{x}_{ij}, t_k)$ represents the concentration of the component in the cell (i, j) at point $\mathbf{x}_{ij} = (y_i, z_j)$ and time t_k , and $\phi_0 \in [0; 1]$ is a suitable evolutionary coefficient. Fig. 1 shows the pattern of cells involved in the evolutionary rule for the cell (i, j) .

Clearly, to regulate the process according to a given diffusivity D , a proper discretization in space and time is required. As shown in the Appendix, the grid dimension Δx and the time step Δt of the cellular automaton must satisfy the following relationship:

$$D = \frac{1 - \phi_0}{4} \frac{\Delta x^2}{\Delta t} \quad (3)$$

The deterministic value $\phi_0 = 1/2$ usually leads to a good accuracy of the automaton. However, the local stochastic effects in the mass transfer can be easily taken into account by assuming ϕ_0 as random variable. The probability distribution of this parameter does not represent a critical point, and very simple triangular distributions may be successfully adopted [2]. Clearly, symmetrical functions should be adopted to avoid directionality effects in the stochastic model. However, skewed distributions towards the higher values of ϕ_0 could also be applied to simulate the local increase in the rate of mass diffusion in the cracked regions. In this way, the interaction between the diffusion process and the mechanical behavior of the damaged structure can be effectively taken into account. More details can be found in [2].

2.3. Modeling structural damage

Damaging processes in concrete structures may involve a reduction of the effective resistant area of the materials, due for example to corrosion of the steel reinforcement and cracking, spalling and delamination of the concrete matrix [8]. In the proposed approach, this kind of structural damage is modeled by introducing a degradation law of the effective resistant areas for the concrete matrix, steel bars, and prestressing cables. The amount of degradation is then described by means of dimensionless *damage indices* δ_c , δ_s , and δ_p , for concrete, reinforcing steel, and prestressing steel respectively, which provide a direct measure of the damage level of the materials within the range [0; 1].

The time evolution of the damage indices is related to the corresponding evolution of the diffusive process. For example, when deterioration is induced by aggressive agents, such as chlorides, the rate of damage depends, among other factors, on the level of concentration of the substances which diffuse inside the structure. This dependence is in general very complex, and the available information about environmental agents and material characteristics is usually not sufficient for a detailed modeling. However, despite such complexities, very simple degradation models may be successfully adopted for an overall evaluation of the lifetime structural performance. In the proposed approach, the damage indices $\delta = \delta(\mathbf{x}, t)$ at point $\mathbf{x} = (y, z)$ and time t are correlated to the diffusion process by assuming, for each material, a linear relationship between the rate of damage and the mass concentration $C = C(\mathbf{x}, t)$ of the aggressive agent [2]:

$$\frac{\partial \delta_c(\mathbf{x}, t)}{\partial t} = \frac{C(\mathbf{x}, t)}{C_c \Delta t_c} \quad (4)$$

$$\frac{\partial \delta_s(\mathbf{x}, t)}{\partial t} = \frac{C(\mathbf{x}, t)}{C_s \Delta t_s} \quad (5)$$

$$\frac{\partial \delta_p(\mathbf{x}, t)}{\partial t} = \frac{C(\mathbf{x}, t)}{C_p \Delta t_p} \quad (6)$$

where C_c , C_s , and C_p represent the values of constant concentration $C(\mathbf{x}, t)$ which lead to a complete damage of the materials after the time periods Δt_c , Δt_s , and Δt_p , respectively. In addition, for each material, the initial condition $\delta(\mathbf{x}, t_0) = 0$

with $t_0 = \max\{t \mid C(\mathbf{x}, t) \leq C_{cr}\}$ is assumed, where C_{cr} is a critical threshold of concentration.

2.4. Structural analysis of R/C and P/C cross-sections

The cross-sectional formulation of structural analysis assumes the linearity of concrete strain field and neglects the bond-slip of reinforcement. Based on these hypotheses, the vectors $\mathbf{r} = \mathbf{r}(t) = [N \ M_z \ M_y]^T$ of the stress resultants (axial force N and bending moments M_z and M_y), and of the generalized strains $\mathbf{e} = \mathbf{e}(t) = [\varepsilon_0 \ \chi_z \ \chi_y]^T$ (axial elongation ε_0 and bending curvatures χ_z and χ_y), can be related, at each time instant t , as follows [14]:

$$\mathbf{r}(t) + \mathbf{r}_p(t) = \mathbf{H}(t) \mathbf{e}(t). \quad (7)$$

The stiffness matrix $\mathbf{H} = \mathbf{H}(t)$ and the vector of nodal forces equivalent to prestressing $\mathbf{r}_p = \mathbf{r}_p(t)$ are derived at each time instant by integration over the area of the damaged cross-section:

$$\mathbf{H}(t) = \mathbf{H}_c(t) + \mathbf{H}_s(t) + \mathbf{H}_p(t) \quad (8)$$

$$\mathbf{H}_c(t) = \int_{A_c(x)} E_c(y, z, t) \mathbf{b}(y, z)^T \mathbf{b}(y, z) [1 - \delta_c(y, z, t)] dA \quad (9)$$

$$\mathbf{H}_s(t) = \sum_m E_{sm}(t) \mathbf{b}_m^T \mathbf{b}_m [1 - \delta_{sm}(t)] A_{sm} \quad (10)$$

$$\mathbf{H}_p(t) = \sum_n E_{pn}(t) \mathbf{b}_n^T \mathbf{b}_n [1 - \delta_{pn}(t)] A_{pn} \quad (11)$$

$$\mathbf{r}_p(t) = - \sum_n E_{pn}(t) \mathbf{b}_n [1 - \delta_{pn}(t)] A_{pn} \varepsilon_{p0n} \quad (12)$$

where the symbols “ m ” and “ n ” refer to the m th reinforcing bar located at $\mathbf{x}_m = (y_m, z_m)$, and to the n th prestressing cable located at $\mathbf{x}_n = (y_n, z_n)$, respectively, $E_c = E_c(y, z, t)$, $E_{sm} = E_{sm}(t)$, and $E_{pn} = E_{pn}(t)$ are the secant moduli of the materials, ε_{p0n} is the prestressing strain, and $\mathbf{b}(y, z) = [1 \ -y \ z]$. In the following the two-dimensional case with $M = M_z \neq 0$ and $M_y = 0$ is considered.

The evaluation of the above integral quantities requires the constitutive laws of the materials to be defined. For concrete, the stress–strain diagram is described by the Saenz’s law in compression and by an elastic perfectly plastic model in tension. By denoting with f_c the compression strength of the material, the following parameters are assumed: tension strength $f_{ct} = 0.25|f_c|^{2/3}$; initial modulus $E_{c0} = 9500|f_c|^{1/3}$; peak strain in compression $\varepsilon_{c0} = -0.20\%$; strain limit in compression $\varepsilon_{cu} = -0.35\%$; strain limit in tension $\varepsilon_{ctu} = 2f_{ct}/E_{c0}$. For reinforcing steel, the stress–strain diagram is described by an elastic perfectly plastic model in both tension and compression with yielding strength f_{sy} , elastic modulus $E_s = 206$ GPa, and strain limit $\varepsilon_{su} = 1.00\%$. For prestressing steel, the stress–strain diagram is described by an elastic perfectly plastic model in both tension and compression with yielding strength f_{py} , elastic modulus $E_p = 200$ GPa, and strain limit $\varepsilon_{pu} = \varepsilon_{p0} + 1.00\%$.

Table 1
Probability distributions and their parameters

Random variable ($t = t_0$)	Distribution type	μ	σ
Concrete strength, f_c	Lognormal	$f_{c,nom}$	5 MPa
Reinforcing steel strength, f_{sy}	Lognormal	$f_{sy,nom}$	30 MPa
Prestressing steel strength, f_{py}	Lognormal	$f_{py,nom}$	100 MPa
Coordinates of the nodal points, (y_r, z_r)	Normal	$(y_r, z_r)_{nom}$	5 mm
Coordinates of the reinforcing bars, (y_m, z_m)	Normal	$(y_m, z_m)_{nom}$	5 mm
Coordinates of the prestressing cables, (y_n, z_n)	Normal	$(y_n, z_n)_{nom}$	5 mm
Diameter of the reinforcing bars, \varnothing_m	Normal ^a	$\varnothing_{m,nom}$	$0.10 \varnothing_{m,nom}$
Diameter of the prestressing cables, \varnothing_n	Normal ^a	$\varnothing_{n,nom}$	$0.10 \varnothing_{n,nom}$
Cables prestressing, σ_{p0n}	Normal ^a	$\sigma_{p0n,nom}$	$0.10 \sigma_{p0n,nom}$
Diffusivity coefficient, D	Normal ^a	D_{nom}	$0.10 D_{nom}$
Concrete damage rate, q_c	Normal ^a	$q_{c,nom}$	$0.30 q_{c,nom}$
Reinforcing steel damage rate, q_s	Normal ^a	$q_{s,nom}$	$0.30 q_{s,nom}$
Prestressing steel damage rate, q_p	Normal ^a	$q_{p,nom}$	$0.30 q_{p,nom}$

^a Truncated distributions with non negative outcomes are adopted in the simulation process.

2.5. Probabilistic modeling for lifetime assessment

The probabilistic analysis is carried out by Monte Carlo simulation. The probabilistic model assumes as random variables the material strengths f_c , f_{sy} , and f_{py} , the coordinates (y_r, z_r) of the nodal points $r = 1, 2, \dots$ which define the two-dimensional model of the concrete cross-section, the coordinates (y_m, z_m) and the diameter \varnothing_m of the reinforcing bars $m = 1, 2, \dots$, the coordinates (y_n, z_n) and the diameter \varnothing_n of the prestressing cables $n = 1, 2, \dots$, the initial prestressing σ_{p0n} , the diffusion coefficient D , and the damage rates $q_c = (C_c \Delta t_c)^{-1}$, $q_s = (C_s \Delta t_s)^{-1}$, and $q_p = (C_p \Delta t_p)^{-1}$. These variables are assumed to be uncorrelated and having the probabilistic distribution with the mean μ and standard deviation σ values listed in Table 1 [3].

The sampling error associated with the simulation process is reduced by the antithetic variables technique, while a posteriori estimation on the goodness of the sample size s is based on a monitoring of the statistical parameters, mean value $\mu = \mu(t, s)$ and standard deviation $\sigma = \sigma(t, s)$ of the random variables under investigation, for each time instant t of interest.

2.6. Regression analysis and sensitivity factors

In the subsequent applications, the time evolution of the probabilistic performance will be analyzed with reference to proper indicators of the nonlinear structural behavior. Let X denote a parameter of the structural problem, and Y a performance indicator. In order to investigate the effects of the uncertainty associated with each parameter X on each indicator Y , the following standard variates are introduced:

$$\xi(t) = \frac{|X(t) - \mu_X(t)|}{\sigma_X(t)} \quad (13)$$

$$\eta(t) = \frac{|Y(t) - \mu_Y(t)|}{\sigma_Y(t)} \quad (14)$$

where μ_X , σ_X , and μ_Y , σ_Y , are the time-variant mean value and standard deviation of the random variables X and Y , respectively. Based on these variates, a set of time-variant least

squares linear regression is performed on the data samples obtained from the simulation in the following form:

$$\eta(t) = \alpha_{XY}(t)\xi(t) + \alpha_{0,XY}(t). \quad (15)$$

In this way, the regression coefficients α_{XY} are assumed as a time-dependent measure of the sensitivity of the dependent variable Y with respect to the independent variable X .

3. Lifetime performance of the Certosa cable-stayed bridge

3.1. Characteristics of the bridge

This section is based on material presented by the authors in [5]. The Certosa cable-stayed bridge was designed by Francesco Martinez Y Cabrera [15]. The total length of the Certosa bridge is 180 m, with a central span of 90 m and two lateral spans of 45 m, as shown in Fig. 2a. The bridge deck is a five cells box girder, 19.80 m wide and 26.7° skewed with respect to the road axis, and its transversal cross-section has a depth varying from 1.40 m to 1.80 m (Fig. 2b, c). Along its span the box is stiffened by a set of transversal beams (Fig. 2d). Such beams end with two short cantilevers to which the stays are anchored. The deck and the beams are prestressed with cables made up of 14 and 19 strands of 0.6 inches. The pylons of the cable-stayed bridge are 19.00 m high and have a rectangular cross-section, varying along the height from 1.14×2.00 m at the top to 1.14×2.50 m at the bottom (Fig. 2d). The tapered shape of the frontal view finishes in two corbels which were planned to lift the bridge during the erection stage. The ends of the pylons carry the steel devices used to anchor the stays. There are in total three seats consisting of steel boxes which make it possible to anchor the stays leaving them crossed, but not intersected, on the same plane. Each pylon has 3+3 sets of stays, skewed with respect to the horizontal plane, as shown in Fig. 2d.

3.2. Structural repair interventions

The Certosa cable-stayed bridge was opened in 1989 (Fig. 3a). After about fifteen years of service, the Milan

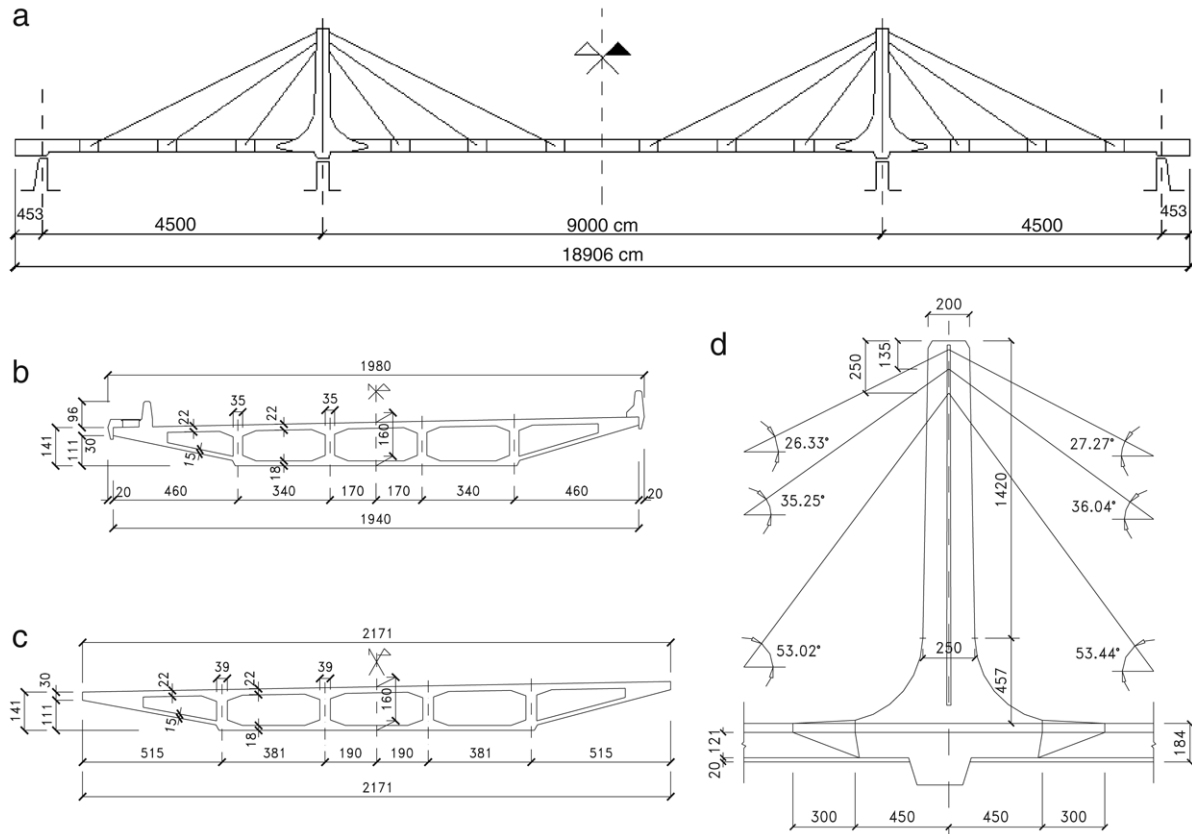


Fig. 2. Certosa cable-stayed bridge. (a) Main dimensions of the bridge. (b–c) Main dimensions of the bridge deck: (b) straight cross-section; (c) skewed cross-section. (d) Main dimensions of the pylons.

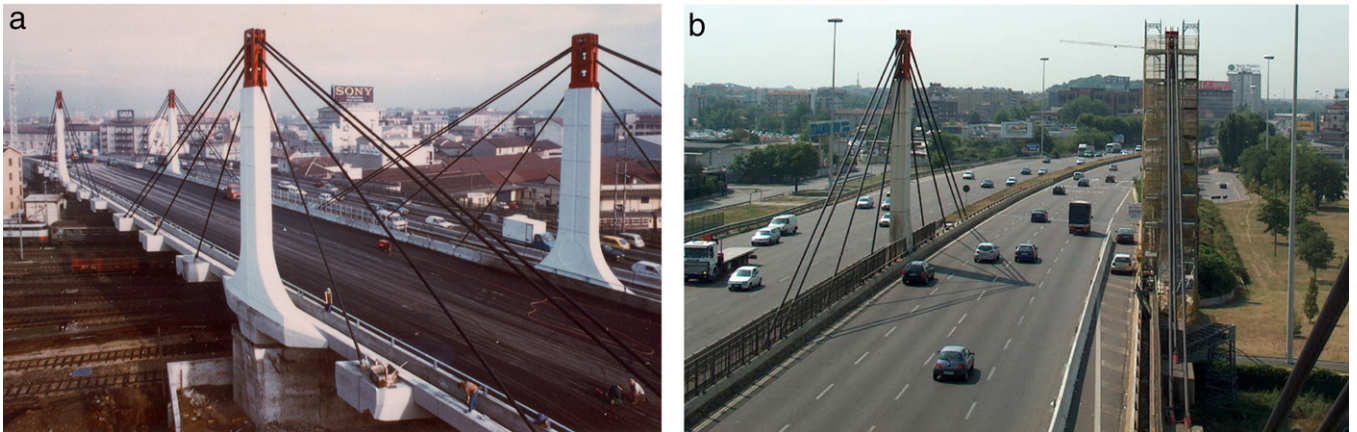


Fig. 3. View of the Certosa bridge (a) at the end of construction, and (b) during repair activities.

Municipality decided for a general and detailed inspection of the bridge (Fig. 3b). This inspection revealed some damage, especially at the bottom part of the pylons, induced by the interaction with the surrounding environment. For this reason, a structural repair of the pylons was decided. After a strong sandblasting cleaning, the main cracks have been carved up to the basis of the crack and then sutured with thixotropic, anti-shrinkage, polypropylene fiber reinforced high strength mortar. The small cracks and the segregation zones have been repaired with high adhesion cement mortar, added with small

polyvinylalcohol fibers. The whole skin surfaces have been protected with high adhesion, high elasticity cement mortar, reinforced with double or simple skin mesh. This protection contributes to counteracting the restart of carbonation and it is transpiring outward and waterproof inward. The final surface was painted with a silicate non-pellicular paint. In this way, future diffusive attacks of external aggressive agents are prevented. More detailed information about these repair interventions can be found in [5].

evaluated up to 50 years by considering two scenarios. In the first one the structure is left free to undergo damage without any intervention. In the second one the effects of the rehabilitation, carried out after fifteen years of service, are taken into account by (a) assuming an undamaged state for the restored layer of the concrete cover and (b) placing a diffusive barrier along the boundary of the cross-section in such a way that diffusion of aggressive agents from outside is stopped and future damage can be induced only by the agent already existing inside the structure. To this aim, the cellular automaton model shown in Fig. 4b is updated during the analysis of the restored structure by changing the material properties of the outer layer of concrete cells and removing the external source of aggressive agent.

With reference to a nominal diffusivity coefficient $D = 10^{-11} \text{ m}^2/\text{s}$ for concrete, the diffusion process associated with the two investigated scenarios, without and with rehabilitation intervention, is described by the maps of concentration shown in Fig. 5. The direct comparison of the concentration maps in Fig. 5a and b highlights the high effectiveness of rehabilitation intervention with regards to the limitation of the diffusive attack of the aggressive agent.

To evaluate the mechanical damage induced by diffusion, the damage rates in the materials $q_c = (C_c \Delta t_c)^{-1}$, and $q_s = (C_s \Delta t_s)^{-1}$, need to be defined. Since no quantitative information is available on these parameters, the damage model has been set in such a way that the damage observed during inspection is fully developed after fifteen years of lifetime. Based on this criterion, the time evolution of mechanical damage is evaluated by assuming $C_c = C_s = C_0$, $\Delta t_c = 25$ years, $\Delta t_s = 50$ years, and $C_{cr} = 0$. Several parameters could be adopted as suitable measures of structural performance. As an example, Fig. 6 shows the time evolution of the yielding value m_y of the dimensionless bending moment $m = M/(|f_c|A_{c0}h)$ under the axial force $n = N/(|f_c|A_{c0}) = -0.201$, where $A_{c0} = bh$ is the area of the undamaged cross-section, and $N = -20$ MN. This diagram shows that

Fig. 4. Cross-section at the base of the pylons. (a) Model, dimensions and reinforcement. (b) Grid of the automaton and location of the aggressive agent.

3.3. Prediction of lifetime performance

The attention is focused on the cross-section at the base of the pylons, where the most evident traces of deterioration were present. Such a cross-section has main nominal dimensions $b = 1.14$ m and $h = 2.50$ m, and is reinforced with 86 bars having nominal diameter $\varnothing = 26$ mm (Fig. 4a). The nominal values of the material strengths are $f_c = -35$ MPa, and $f_{sy} = 500$ MPa.

In the investigated scenarios, the cross-section is assumed to be subjected to a diffusive attack from an environmental aggressive agent, which is considered to be located along the whole external perimeter with constant concentration $C(t) = C_0$ (Fig. 4b). The time-variant performance of the pylons is

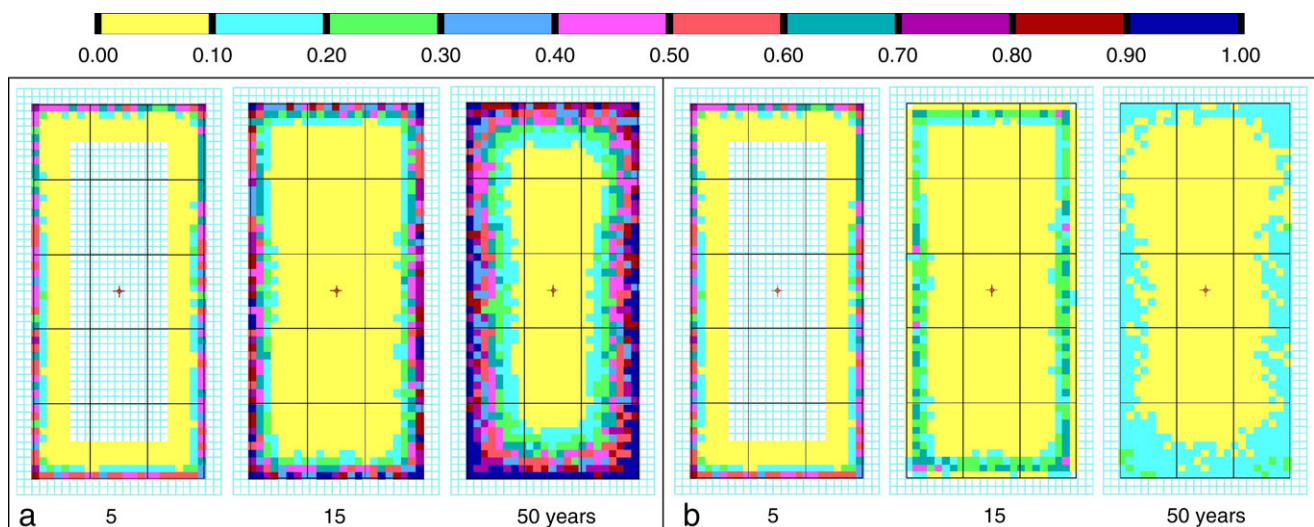


Fig. 5. Maps of concentration $C(t)/C_0$ of the aggressive agent after 5, 15, and 50 years from the initial time of diffusion penetration. (a) Damaged structure. (b) Rehabilitated structure.

